Hole Transport Molecules in High T_g Polymers: Their Effect on the Performance of Organic Light-Emitting Diodes

F. Santerre, I. Bedja, and J. P. Dodelet*

INRS-Énergie et Matériaux, C.P.1020, Varennes, Quebec, Canada J3X 1S2

Y. Sun, J. Lu, and A. S. Hay

Department of Chemistry, McGill University, Montreal, Quebec, Canada H3A 2K6

M. D'Iorio

IMS, National Research Council, Ottawa, Ontario, Canada K1A 0R6

Received November 21, 2000. Revised Manuscript Received February 28, 2001

Two high T_g transparent polymers, A435 and CH, have been synthesized to be used as host materials for TPD, a hole transport molecule that is morphologically unstable when vacuum-sublimed as a thin film. A435 forms solid solutions with TPD in all proportions while TPD is only soluble in CH up to about 30 wt %. At higher contents in CH, TPD forms microscopic clusters. Films containing up to 75 wt % TPD in A435 or CH are morphologically stable when heated at 100 °C for 72 h. OLED devices have been made using variable TPD contents in A435 or CH as a hole transport layer and Alq_3 as an electroluminescent and electron transport layer. The best OLED performance is obtained for 75 wt % TPD in A435 ($L_{max} \sim 3500$ cd/m^2; $\eta_{max} \sim 0.8\%$) and in CH ($L_{max} \sim 6000$ cd/m^2; $\eta_{max} \sim 1.7\%$). The difference in performance has been mainly attributed to the electron transport capability of A435, which is not an electrically inactive host polymer like CH. In devices made with A435, electrons are able to reach the ITO electrode where they neutralize without participating in the electroluminescence of the device. When this electron leakage is blocked with a thin CuPc layer, L_{max} and η_{max} of devices made with A435 + TPD or CH + TPD become practically identical. Device performance is therefore indifferent to the particular physical state (solid solution or microclusters) of the hole transport molecules in the host polymer. The electron transport capability of A435 has been demonstrated using a device comprising a first layer of pure A435 spin-coated on top of a layer of high T_g polymer, STPD-QP, showing bipolar transport properties and luminescence in the blue.

Introduction

TPD (*N*,*N*′-diphenyl-*N*,*N*′-di-(*m*-tolyl)-*p*-benzidine (Figure 1) has been used extensively as a molecular hole transport layer in the fabrication of organic light-emitting diodes (OLEDs).[1] It is one of the hole transport materials with high hole drift mobility, which was developed for charge transport layers in xerography.[2] Layers of TPD obtained by vacuum sublimation are highly amorphous, a state of the material required for performing OLED devices. However, TPD, which has a low glass transition temperature (T_g) of about 60 °C, has a propensity to crystallize upon aging.[3] Because of local Joule heating in operating OLEDs, the crystallization of TPD has also been invoked[4,5] as one of the most likely origins of the degradation of the devices by providing nonradiative trapping sites.[6] A large thermal expansion of TPD associated with its glass transition has also been blamed for the degradation of the interface between TPD and Alq_3 (8-hydroxyquinoline aluminum) (Figure 1), the archetype of the electroluminescent and electron transport materials.[7]

Various solutions have been proposed to prevent the physical changes occurring in TPD in the neighborhood of its T_g. Mixing TPD with another hole transport molecule greatly improved the morphological stability of the film.[8] A second solution was the use of arylamine-based hole transport molecules characterized by a higher T_g than TPD. Molecular hole transport materials with T_g from 75 to 152 °C have been used for that purpose.[9−16] To circumvent the morphological changes

* To whom correspondence should be addressed.

(1) Chen, C. H.; Shi, J.; Tang, C. W. *Macromol. Symp.* **1997**, *125*, 1.
(2) Borsenberger, P. M.; Weiss, D. S. *Organic Photoreceptors for Xerography*; Marcel Dekker: New York, 1998.
(3) Han, E. M.; Do, L. M.; Yamamoto, N.; Fujihira, M. *Mol. Cryst. Liq. Cryst.* **1995**, *267*, 411.
(4) Adachi, C.; Tsutsui, T.; Saito, S. *Appl. Phys. Lett.* **1990**, *56*, 799.
(5) Han, E. M.; Do, L. M.; Niidome, Y.; Fujihira, M. *Chem. Lett. (Jpn.)* **1994**, 969.
(6) Salbaneck, J. *Ber. Bunsen-Ges. Phys. Chem.* **1996**, *100*, 1667.
(7) Fenter, P.; Schreiber, F.; Bulovic, V.; Forrest, S. R. *Chem. Phys. Lett.* **1997**, *277*, 521.
(8) Sato, Y.; Kanai, H. *Mol. Cryst. Liq. Cryst.* **1994**, *253*, 141.

10.1021/cm0009221 CCC: $20.00
Published on Web 04/10/2001

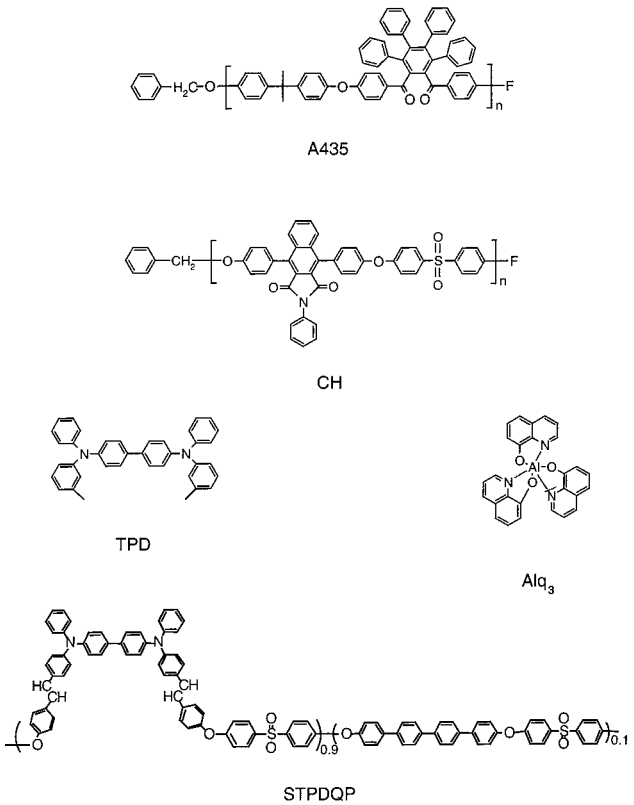

Figure 1. Molecular structure of two high T_g host polymers CH and A435 and their respective precursors, **1** and **2**; molecular structure of an active high T_g polymer, STPD-QP, and two active molecules, TPD and Alq_3.

of the hole transport layer, polymers with arylamine-based functionality have also been synthesized. In most of the cases, the arylamine-based functionality is incorporated in the polymer main chain.[17−25] Some of these polymers have a T_g of up to 215 °C.[25] Pendent-arylamine-based hole-transporting polymers have also been synthesized. Some of these polymers have a T_g in the range of 130−150 °C.[26−29] Pendent-arylamine-based hole-transporting polymers with various contents of trimethoxysilane have also been prepared and cross-linked to glass.[30]

Another approach for improving the resistance to morphological changes of the hole transport layer is obtained by dissolving TPD in a high T_g transparent host polymer. This is the approach followed in this work. It uses two high T_g host polymers: A435 (T_g = 252 °C) and CH (T_g = 323 °C). The molecular structures of A435 and CH are presented in Figure 1. In this paper, the following will be demonstrated: (i) the solubility of TPD in high T_g host polymers greatly varies from A435 to CH, but the presence of the host polymer always impedes TPD crystallization; (ii) it is possible to use a host polymer + TPD as a hole transport layer in OLEDs (the best performing devices have a TPD content around 75 wt % and display maximum luminance's of several thousand cd/m^2); (iii) for the same hole transport molecule, the performance depends however upon the host polymer used; (iv) a copper phthalocyanine (CuPc) layer vacuum-sublimed between the transparent anode and the hole transport layer drastically improves the performance of the devices made with A435 + TPD. While we were trying to explain this behavior, we discovered that A435 is not an electrically inactive host polymer like CH but A435 displays some electron transport properties.

Experimental Section

Synthesis of High T_g Amorphous Polymers. Three high T_g amorphous polymers were used in this work. They are as follows:

CH: poly(imidoaryl ether sulfone); T_g = 323 °C

A435: poly(aryl ether ketone); T_g = 252 °C

STPD-QP: T_g = 253 °C

The molecular structure of these polymers is displayed in Figure 1. The detailed experimental procedure used to synthesize these polymers is given in the Supporting Information section. (References 31−33 are related to the detailed procedure).

Fabrication and Characterization of the EL Devices. ITO substrates (15 Ω/□ from Applied Films Corporation) were cleaned with methanol and then patterned by a rapid acid etching with Zn and HCl to obtain the anode of the devices. Patterned ITO substrates were cleaned in an acidic bichromate solution for 30 min and then rinsed with deionized water and hot acetone before being dried under N_2. All the layers containing TPD were obtained by dissolving the molecular hole transport molecule in one of the two transparent host polymers (A435 or CH) and then by spin coating (Speciality Coating Systems; model P6204) the filtered solutions (1.0-μm filters from Whatman) at 1000 rpm for 10 s. The thickness of the hole transport layers was around 80 nm unless otherwise specified. The solvent used to dissolve A435 + *x*TPD is a 2:1 mixture, in volume, of dichloromethane and toluene. It has been demonstrated[34] that the layers obtained with this solvent

(9) Itano, K.; Ogawa, H.; Shirota, Y. *Appl. Phys. Lett*. **1998**, *72*, 636.
(10) Van Slyke, S. A.; Chen, C. H.; Tang, C. W. *Appl. Phys. Lett*. **1996**, *69*, 2160.
(11) Shi, J.; Tang, C. W. *Appl. Phys. Lett*. **1997**, *70*, 1665.
(12) Tokito, S.; Tanaka, H.; Noda, K.; Okada, A.; Taga, Y. *Appl. Phys. Lett*. **1997**, *70*, 1929.
(13) Thelakkat, M.; Schmidt, H. W. *Adv. Mater*. **1998**, *10*, 219.
(14) Tanaka, H.; Tokito, S.; Taga, Y.; Okada, A. *J. Chem. Soc. Chem. Commun*. **1996**, 2175.
(15) Kuwabara, Y.; Ogawa, H.; Inada, H.; Noma, N.; Shirota, Y. *Adv. Mater*. **1994**, *6*, 677.
(16) O'Brien, D.; Burrows, P. E.; Forrest, S. R.; Koene, B. E.; Loy, D.; Thompson, M. E. *Adv. Mater*. **1998**, *10*, 1108.
(17) Hosokawa, C.; Kawasaki, N.; Sakamoto, S.; Kusumoto, T. *Appl. Phys. Lett*. **1992**, *61*, 2503.
(18) Kim, D. U.; Tsutsui, T.; Saito, S. *Polymer* **1995**, *36*, 2481.
(19) Hörhold, H. H.; Rost, H.; Teuschel, A.; Kreuder, W.; Spreitzer, H. *Proc. SPIE* **1997**, *3148*, 139.
(20) Adachi, C.; Hibino, S.; Koyoma, T.; Taniguchi, Y. *Jpn. J. Appl. Phys*. **1997**, *36*, L827.
(21) Yamamori, A.; Adachi, C.; Koyama, T.; Taniguchi, Y. *Appl. Phys. Lett*. **1998**, *72*, 2147.
(22) Liu, Y.; Liu, M. S.; Li, X. C.; Jen, A. K. Y. *Chem. Mater*. **1998**, *10*, 3301.
(23) Schmitz, C.; Thelakkat, M.; Schmidt, H. W. *Adv. Mater*. **1999**, *11*, 821.
(24) Yu, G.; Liu, Y.; Wu, X.; Zheng, M.; Bai, F.; Zhu, D.; Jin, L.; Wang, M.; Wu, X. *Appl. Phys. Lett*. **1999**, *74*, 2295.
(25) Liu, Y.; Ma, H.; Jen, A. K. Y. *Chem. Mater*. **1999**, *11*, 27.
(26) Bellmann, E.; Shaheen, S. E.; Thayumanavan, S.; Barlow, S.; Grubbs, R. H.; Marder, S. R.; Kippelen, B.; Peyghambarian, N. *Chem. Mater*. **1998**, *10*, 1668.
(27) Bellmann, E.; Shaheen, S. E.; Grubbs, R. H.; Marder, S. R.; Kippelen, B.; Peyghambarian, N. *Chem. Mater*. **1999**, *11*, 399.
(28) Shaheen, S. E.; Jabbour, G. E.; Kippelen, B.; Peyghambarian, N.; Anderson, J. D.; Marder, S. R.; Armstrong, N. R.; Bellmann, E.; Grubbs, R. H. *Appl. Phys. Lett*. **1999**, *74*, 3212.
(29) Jiang, X.; Sen, L.; Liu, M. S.; Ma, H.; Jen, A. K. Y. *Appl. Phys. Lett*. **2000**, *76*, 2985.
(30) Bellmann, E.; Jabbour, G. E.; Grubbs, R. H.; Peyghambarian, N. *Chem. Mater*. **2000**, *12*, 1349.
(31) Singh, R.; Hay, A. S. *Macromolecules* **1992**, *25*, 1017.

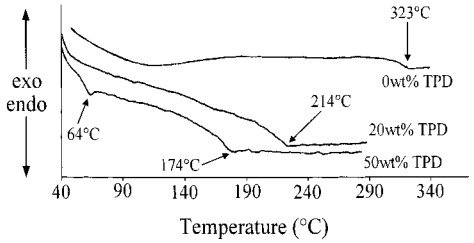

Figure 2. Differential scanning calorimetry of CH + *x*TPD.

mixture are very flat while those obtained from solutions in dichloromethane show thickness inhomogeneities, especially at low hole transport content. Various solutions containing A435 + *x*TPD, with $x = 25-90$ wt % have been used. The spin-coated solutions always consisted of 20 mg of solute in 3 mL of solvent. The high T_g host polymer CH is not soluble in the dichloromethane−toluene solvent mixture. Therefore, pure dichloromethane was used to dissolve CH + *x*TPD. Various solutions containing CH + *x*TPD, with $x = 25-90$ wt %, have been used. It will be shown in the Results section that these layers display some thickness inhomogeneities. STPD-QP was spin-coated from filtered solutions in chloroform (9 mg/3 mL) at 700 rpm for 10 s. All surface morphologies have been measured by atomic force microscopy (AFM) using a Nanoscope III microscope from Digital Instruments.

Alq_3 was vacuum-sublimed at a residual pressure of about 1.5×10^{-5} mbar. After an initial degassing for 15 min at 200 °C, Alq_3 was heated to about 230 °C and Alq_3 films were grown for 20 s. The thickness of the Alq_3 films was about 40 ± 10 nm. The devices were completed by a vacuum deposition at about 1.5×10^{-6} mbar (in a different system) of a Mg cathode 0.2−0.3-μm-thick. Five OLEDs were fabricated at the same time on the same ITO-covered glass plate. The dimensions of each OLED were 2 × 13 mm. Current−voltage and luminance−voltage curves were recorded at the same time in an Ar atmosphere. The voltage source was an EG&G Model 175 Universal Programmer. Luminance was measured with a Tektronix Lumacolor II photometer, Model J18. Electroluminescence spectra were recorded using a monochromator (ISA Instruments) and a photomultiplier and a photometer (Pacific Precision Instruments, Model 126). The apparent quantum efficiency of the OLEDs was calculated according to the following relation,

$$\eta = 4\pi qL\lambda_{per}/(hcKJ) \quad (1)$$

where q is the unit charge, h, c, and π have their usual meaning, L is the luminance, λ_{per} is the barycentric wavelength of the perceived electroluminescence spectrum, K is the photometric to radiometric unit conversion factor (680 Lm/W), and J is the current density in the device.

Results and Discussion

Solubility of TPD in the Host Polymers. The solubility of TPD in the two host polymers (A435 or CH) was measured by DSC. The principle of the method is illustrated in Figure 2 for TPD in CH. This figure presents DSC measurements for three materials: (i) pure CH; (ii) CH + 20 wt % TPD; (iii) CH + 50 wt % TPD. The endothermic reaction detected on curve (i) yields the glass transition temperature of CH at 323 °C. The addition of 20 wt % TPD in CH lowers the glass transition temperature of the solid solution to 214 °C (curve (ii)). Two transitions are visible on curve (iii): the first one at 64 °C corresponds to the glass transition temperature of pure TPD while the second one corresponds to the T_g of the solid solution of TPD in CH. Two phases are therefore produced when 50 wt % TPD is added to CH. This material consists of small TPD clusters dispersed in a saturated solid solution of TPD in CH. Figure 3 describes the T_g changes for A435 and CH with the TPD contents. From Figure 3A one may conclude that TPD is completely miscible with A435, while TPD saturates between 30 and 50 wt % in CH (Figure 3B).

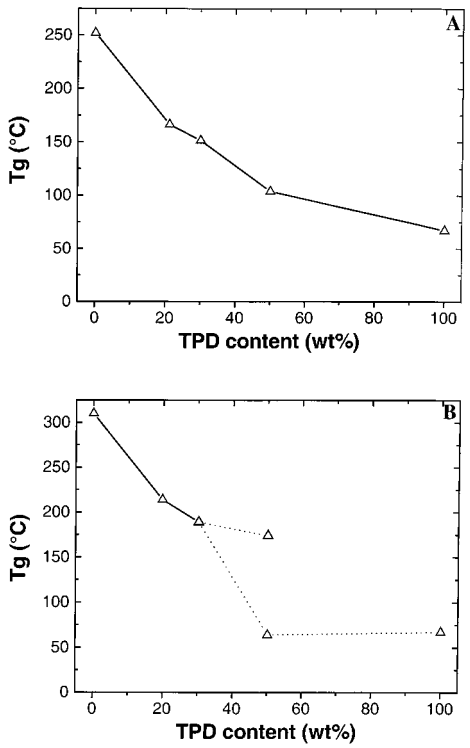

Figure 3. Changes in T_g with the TPD content for (A) A435 and (B) CH.

Annealing of Films Containing TPD in the Host Polymers. Annealing experiments have been performed in a vacuum at 100 °C for 1 h on A435 + *x*TPD and CH + *x*TPD and compared with annealing experiments performed on sublimed TPD. In these conditions, TPD completely crystallized as deduced by the roughness of its entire surface.

Figure 4A depicts the surface morphology before annealing of a film containing 25 wt % TPD in A435. The film is very flat, at least on that vertical scale (each increment is 100 nm). Furthermore, all films containing 25−90 wt % TPD in A435 display the same surface morphology and a similar RMS roughness as defined by

$$R_q = [\Sigma(Z_i - Z_{ave})^2/N_i]^{1/2} \quad (2)$$

where R_q is the standard deviation of the values along the vertical z axis, Z_{ave} is the mean Z value, and N_i is the number of points probed on a 10 × 10 μm^2 square surface. Calculated R_q values for TPD in A435 are given in Table 1. They indicate that the roughness of the films decreases monotonically with the TPD content in A435. All the films containing 25−90 wt % TPD in A435 were heat-treated in a vacuum at 100 °C for 1 h. Only the

(32) Strukelj, M.; Hay, A. S. *Macromolecules* **1992**, *25*, 4271.
(33) Lu, J. P.; Hlil, A. R.; Sun, Y.; Hay, A. S.; Maindron, T.; Dodelet, J. P.; D'Iorio, M. *Chem. Mater.* **1999**, *11*, 2501.
(34) Santerre, F.; Dodelet, J. P.; Sun, Y.; Hlil, A. R.; Hay, A. S.; D'Iorio, M. *Proc. Conf. Imaging Sci. Technol. (IS&T NIP15)* **1999**, 747.

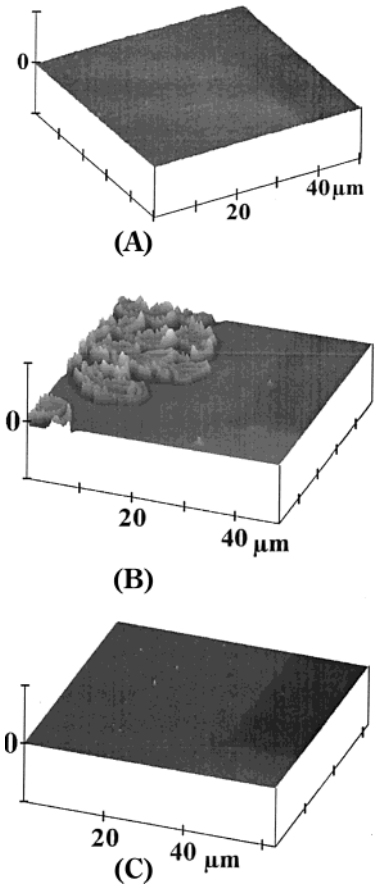

Figure 4. Surface morphology of (A) a film containing 25 wt % TPD in A435; (B) a film containing 90 wt % TPD in A435 after heat treatment in a vacuum at 100 °C for 1 h; (C) a film containing 50 wt % TPD in A435 after heat treatment in a vacuum at 150 °C for 72 h. Vertical increment scale: 100 nm.

Table 1. Roughness (R_q) Analysis for Films of TPD in Two High T_g Host Polymers: A435 and CH

	R_q (nm)			
wt % TPD	A435	CH	wt % TPD	R_q (nm)
25	1.83	1.82	100[a]	4
50	1.56	2.07	100[b]	70
75	1.10	1.42		
90	0.42	0.84		

[a] Freshly vacuum-sublimed TPD film on ITO. [b] After heat treatment of (a) in a vacuum at 100 for 1 h.

surface morphology of A435 + 90 wt % TPD was affected. The result of that annealing treatment is depicted in Figure 4B. It shows the beginning of TPD crystallization at various spots in the film. The films containing 25−75 wt % TPD in A435 were then heat-treated in a vacuum at 150 °C for 72 h. The surface morphology of those films did not change, as is shown in Figure 4C for 50 wt % TPD in A435.

Similar experiments with similar results were also performed on TPD in CH. The difference between the two high T_g host polymers is that the solid solution of TPD saturates before reaching 50 wt % in CH, but TPD is miscible in all proportions in A435. When films containing *x*TPD in CH (with *x* ranging from 25 to 90 wt %) are examined by AFM, the same morphology is observed. Calculated R_q values for films containing TPD in CH are given in Table 1. Despite the fact that, for films containing 75 wt % TPD in CH, TPD clusters are dispersed in a saturated solution of TPD in CH, no TPD clusters are detected by AFM on the film surface. The dimension of these clusters is therefore small (at least smaller than ~1 μm). All the films containing 25−90 wt % TPD in CH were heat-treated in a vacuum at 100 °C for 72 h. Only the surface morphology of CH + 90 wt % TPD was affected. The morphology of CH + *x*TPD films before and after annealing is depicted in the Supporting Information section. In conclusion, it has been shown that it is possible to avoid rapid crystallization of TPD by stabilizing the hole transport molecule in a solid solution in a host polymer, and in some cases, as a dispersion of microscopic clusters of TPD in the host polymers saturated with dissolved TPD.

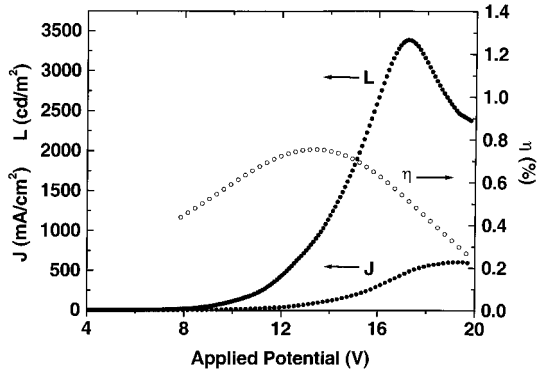

Figure 5. Typical $J-V$, $L-V$, and $\eta-V$ curves for devices using spin-coated A435 + 75 wt % TPD as a hole transport layer.

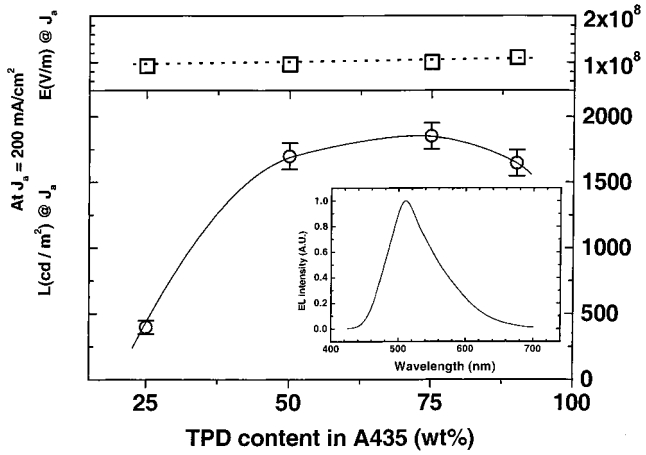

Figure 6. (Top) Applied electric field necessary to obtain $J = 200$ mA/cm^2 in devices using A435 + *x*TPD as a hole transport layer. (Bottom) Changes in luminance with *x*TPD for the same devices. Insert: EL spectrum of these devices.

OLED Devices. *A. OLED Devices Using TPD Molecules in High T_g Polymers.* Figure 5 presents typical current density−applied potential ($J-V$) curves, luminance−applied potential ($L-V$) curves, and apparent quantum efficiency−applied potential ($\eta-V$) curves for devices using A435 + 75 wt % TPD/Alq_3. Figure 6 illustrates changes in luminance with *x*, the TPD content in A435, and also changes in applied electric field (E) with the TPD content in A435, at $J = 200$ mA/cm^2. A typical electroluminescent (EL) spectrum is given in the insert of Figure 6. It is the spectrum of Alq_3.[35]

(35) Tang, C. W.; Van Slyke, S. A.; Chen, C. H. *J. Appl. Phys.* **1989**, *65*, 3610.

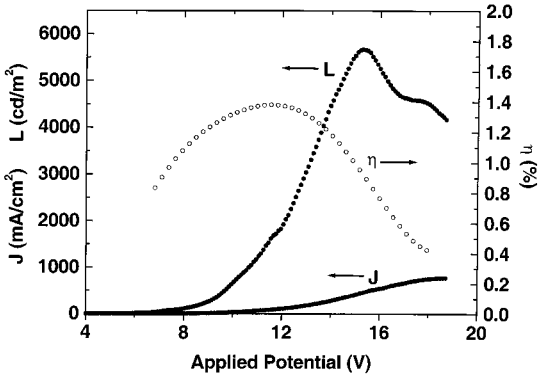

Figure 7. Typical $J-V$, $L-V$, and $\eta-V$ curves for devices using spin-coated CH + 75 wt % TPD as a hole transport layer.

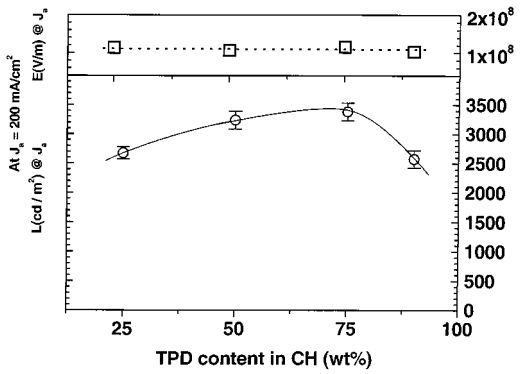

Figure 8. (Top) Applied electric field necessary to obtain $J = 200$ mA/cm^2 in devices using CH + xTPD as a hole transport layer. (Bottom) Changes in luminance with xTPD for the same devices.

Typical $J-V$, $L-V$, and $\eta-V$ curves obtained for devices using CH + 75 wt % TPD/Alq_3 are depicted in Figure 7. Figure 8 illustrates changes in L and E at $J = 200$ mA/cm^2 with the TPD content in CH.

A comparison of Figures 5 and 7 indicates that L_{max} and η_{max} obtained for devices made with CH + 75 wt % TPD are about twice as large as L_{max} and η_{max} obtained for devices made with A435 + 75 wt % TPD. In both cases $J \sim 500$ mA/cm^2. The same difference in luminance is also observed in Figures 6 and 8 at $J = 200$ mA/cm^2. Because the current is held constant in these figures, relative changes in L with the TPD content also represent relative changes in η. The curves in Figures 6 and 8 representing changes in L with the TPD content display a similar behavior: luminance near the maximum luminance are already obtained for $x = 50$ wt % and a broad maximum is reached around $x = 75$ wt %. In the previous section, it was concluded that TPD is soluble in all proportions in A435, while it begins to saturate and form microclusters for $x > \sim 30$ wt %. Therefore, it is clear that the presence of TPD microclusters in TPD-saturated CH is not detrimental to the EL properties of the devices.

If about twice as much luminance is observed for $x \geq 50$ wt % for devices made with CH + TPD than for devices made with A435 + TPD, the luminance ratio reaches ~ 7 for $x = 25$ wt % TPD. In these conditions, TPD is exclusively in solid solution in both polymers. The reason for such a large difference is not attributable to differences in the applied electric field required to obtain $J = 200$ mA/cm^2, which is the same for both host

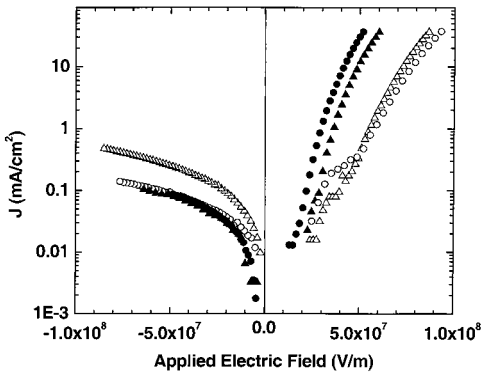

Figure 9. Forward and reverse characteristics of devices made with A435 + 75 wt % TPD (△) and CH + 75 wt % TPD (○). Characteristics of the same devices with an inserted CuPc layer between ITO and A435 + 75 wt % TPD (▲) and ITO and CH + 75 wt % TPD (●).

polymers at all TPD contents studied (see upper part of Figures 6 and 8). We believe that the difference in performance between devices made with A435 + xTPD and CH + xTPD is mainly related to the fact that A435 is a more electrically active host polymer than CH. This is demonstrated in Figure 9. This figure depicts J in direct and reverse biases for devices made with A435 + 75 wt % TPD (△) and CH + 75 wt % TPD (○). It is clear from Figure 9 that J in reverse bias is larger for a device made with A435 + 75 wt % TPD than for a device made with CH + 75 wt % TPD. The former device behaves as a leaky diode. This situation is cured if a thin (~25 nm) layer of copper phthalocyanine (CuPc) is inserted between ITO and the A435 + 75 wt % TPD layer (▲). Insertion of a similar layer between ITO and CH + 75 wt % TPD does not improve the reverse characteristics of these devices (●). In direct bias, the presence of a CuPc layer is beneficial to charge injection in both types of devices. Similarly, the luminance of both devices is also improved as seen in Figure 10. Larger improvements are, however, obtained for devices made with A435 + 75 wt % TPD (Figure 10A, where L_{max} is multiplied by 1.7) than for devices made with CH + 75 wt % TPD (Figure 10B, where L_{max} is only multiplied by 1.1).

B. What Is the Role of CuPc in the Present Devices. It is known that inserting a CuPc layer between ITO and the hole transport layer usually improves the efficiency and stability of OLED devices. Several roles have been attributed to CuPc. They are as follows:

(1) Neutralize the effect of pinholes in the hole transport layer.

(2) Improve the adhesion strength between the hole transport layer relative to the adhesion strength on ITO.[36]

(3) Lower the driving voltage by reducing the effective barrier between ITO and the hole transport layer.[37,38]

(4) Impede hole injection into the hole transport layer, achieving a more balanced electron and hole injection process.[39,40]

(36) VanSlike, S. A.; Chen, C. H.; Tang, C. W. *Appl. Phys. Lett.* **1996**, *69*, 2160.
(37) Kido, J.; Iizumi, Y. *Appl. Phys. Lett.* **1998**, *73*, 2721.
(38) Hill, I. G.; Kahn, A. *J. Appl. Phys.* **1999**, *86*, 2116.
(39) Aziz, H.; Popovic, Z. D.; Hu, N. X.; Hor, A. M.; Xu, G. *Science* **1999**, *283*, 1900.

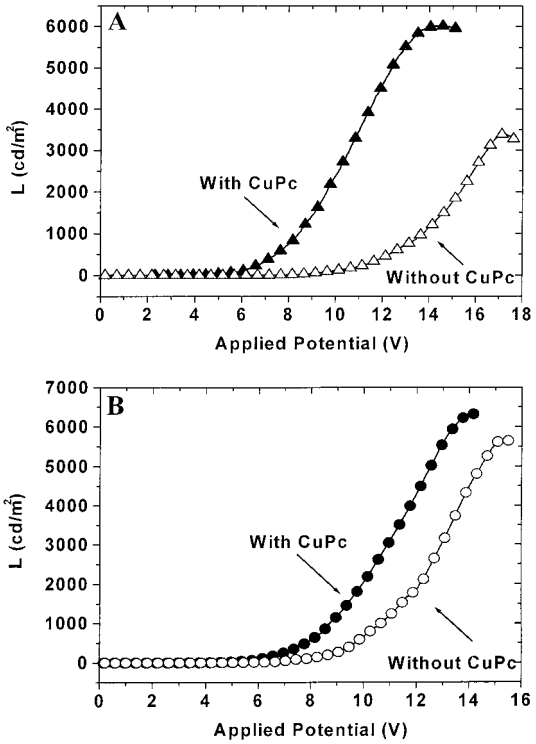

Figure 10. (A) Luminance of a device made with A435 + 75 wt % TPD with and without a CuPc layer between ITO and the hole transport layer; (B) same as (A) but with CH + 75 wt % TPD.

We do not believe that the improvement in performance of the present devices made with A435 + *x*TPD is related to neutralization by CuPc of pinholes in the hole transport layer. This is demonstrated by the following experiments. Three types of devices have been made. They all have the following structure: ITO/A435 + 75 wt % TPD/Alq_3/Mg. In the first type of device (i), the hole transport layer is 87-nm-thick. In the second type of device (ii), the hole transport layer is 110-nm-thick. It is obtained by two successive spin coatings, the first one being 87-nm-thick such as for devices of type (i), followed by a second spin coating, which added 23 nm to the layer thickness. In this process, the first layer is partly dissolved by the solvent during the second spin coating but some A435 + 75 wt % TPD of the first layer remained on ITO because the second coating resulted in a cumulative thickness of 110 nm. In the third type of device (iii), the hole transport layer is obtained by three successive coatings and a cumulative thickness of 120 nm is reached. The morphology of the hole transport layers in devices of type (i)−(iii) is the same.

It is possible and even probable that each layer contains several pinholes but the probability that pinholes in two or three consecutive layers are aligned is very small. Therefore, if there are pinholes in A435 + 75 wt % TPD layers, devices of type (ii) and (iii) should not be influenced by the presence of pinholes, while devices of type (i) should. Figure 11 presents the *L*−*V* curves of devices of types (i)−(iii) relative to the luminance of devices of type (i). The Alq_3 layer and the top Mg electrode of all devices were deposited simultaneously to avoid unnecessary differences. It is clear from

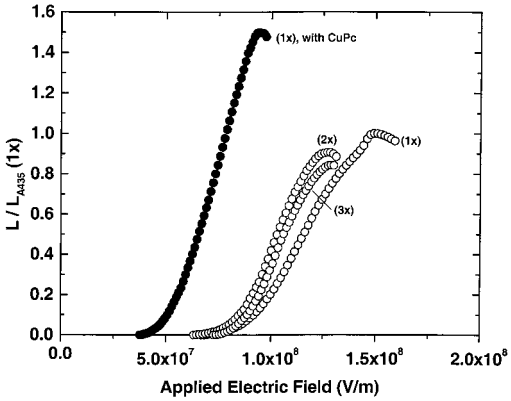

Figure 11. *L*/*L*(1 layer of A435)−*E* curves of devices made with A435 + 75 wt % TPD, where (1x), (2x), and (3x) represent 1, 2, and 3 successive spin-coating steps of the hole transport layer.

Figure 11 that all these devices have a very similar *L*−*V* curve, ruling out a pinhole effect and its neutralization by CuPc. Furthermore, there is only little difference in the luminescence of these devices when the thickness of the hole transport layer varies from 87 to 120 nm. This was expected on the basis of similar results obtained by Burrows and Forrest for sublimed TPD.[41]

Figures 9 and 10 seem to indicate that the insertion of CuPc improves at the same time the current injection and the luminance of the devices. CuPc may therefore lower the driving voltage by reducing the effective barrier between ITO and the hole-transporting layer. This may also be due to better adhesion of the polymer containing TPD on CuPc relative to bare ITO. However, all the above reasons cannot explain why devices based on the same TPD content in A435 or CH behave differently upon addition of a thin layer of CuPc.

In the present case, we believe that A435 is not an electrically inactive host polymer. We believe that the main role of CuPc, which is a hole transport material,[2] is to block the transport of electrons across A435 and their neutralization at the ITO electrode without participating in the device electroluminescence. This will be demonstrated in the following section.

C. Devices Based on STPD-QP. To demonstrate that A435 is able to transport electrons, it was necessary to use STPD-QP (see Figure 1), a high T_g polymer showing some bipolar transport properties, the aryl stilbene moiety of the molecule transporting holes[2] and the quaterphenyl moiety transporting electrons.[42] Figure 12 presents a *L*−*E* curve obtained from a device containing only STPD-QP (37 nm) sandwiched between ITO and Mg electrodes. This polymer displays a faint electroluminescence in the blue (see insert of Figure 12). It originates from the aryl stilbene moiety of the molecule.[31] STPD-QP is only soluble in aggressive solvents such as chloroform.

Figure 12 presents also the *L*−*E* curves for two other devices that comprise a first layer (37 nm) of STPD-QP spin-coated on ITO and a second spin-coated layer, which is either pure A435 (83 nm) or pure CH (55 nm). A435 is spin-coated from its solution in toluene. STPD-

(40) Forsythe, E. W.; Abkowitz, M. A.; Gao, Y. *J. Phys. Chem. B* **2000**, *104*, 3948.

(41) Burrows, P. E.; Forrest, S. R. *Appl. Phys. Lett.* **1994**, *64*, 2285.

(42) Pommerehne, J.; Selz, A.; Book, K.; Koch, F.; Zimmerman, U.; Unterlechner, Chr.; Wendorff, J. H.; Heitz, W.; Bässler, H. *Macromolecules* **1997**, *30*, 8270.

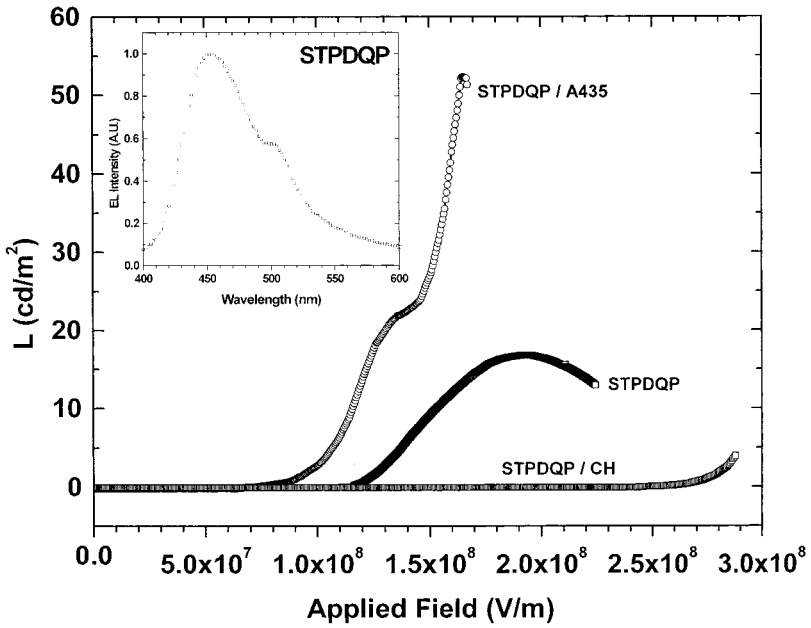

Figure 12. $L-E$ curves of devices of the following structure: ITO/organic/ Mg, with organic being either STPD-QP/A435, STPD-QP alone, or STPD-QP/CH. Insert: EL spectrum of these devices.

QP is not soluble in that solvent. CH is spin-coated from its solution in dichloromethane. STPD-QP is only slightly soluble in that solvent. From Figure 12, it is clear that a second layer of A435 improves the EL of the device, while a second layer of CH kills all device luminescence. A435 is therefore able to transport electrons (the transport of holes would not improve the luminescence of the device), while a layer of CH acts like an insulator.

Electron transport in A435 explains the characteristics observed under reverse bias in Figure 9 for devices with A435 + 75 wt % TPD. Once the leakage of electrons through A435 is blocked by insertion of a CuPc layer, more electrons recombine with holes and improve the luminance of the device to the level of devices made without CuPc but with CH + 75 wt % TPD, as shown in Figure 10.

Conclusions

Two high T_g transparent polymers have been used as hosts for TPD to obtain stable amorphous solid solutions with a high content of these hole transport molecules. It has been shown that TPD is soluble in all proportions in A435. On the other hand, a dispersion of TPD clusters occurs in CH when the content of that hole transport molecule is increased above ~30 wt %. Films of ~80-nm-thick of A435 and CH containing up to 75 wt % TPD are morphologically stable when heat-treated at 100 °C for 72 h. These films have been used to obtain OLED devices of the following structure: ITO/host polymer + xTPD/Alq_3/Mg; x has been varied from 25 to 90 wt %. For both high T_g host polymers, L_{max} and η_{max} are found at x = 75 wt % TPD. L_{max} of about 3500 cd/m^2 (η_{max} ~ 0.8%) are obtained for devices made with A435 + 75 wt % TPD, while L_{max} of about 6000 cd/m^2 (η_{max} ~ 1.6%) are obtained for devices based on CH + 75 wt % TPD. A thin layer of CuPc between ITO and the hole transport layer increases the luminance of A435 + TPD based devices to the level of those obtained for CH + TPD based devices made without CuPc. The main effect of CuPc on the performance of devices made with A435 + TPD is related to the electron transport blocking properties of the CuPc molecular layer. It has indeed been demonstrated that A435 is not an electrically inactive host polymer like CH. A435 is able to transport electrons that, in the absence of CuPc, may neutralize at the ITO electrode and are therefore lost for the electroluminescence of the device.

The reason A435 shows some electron transport properties is still unknown. We believe that it is related to the aryl ketone part of the molecule because the benzoyl group is strongly electron-withdrawing and many electron transport molecules have functionalities characterized by strong dipole moments.[2] Most of the materials exhibiting electron transport capabilities contain nitrogen heterocycles such as oxadiazoles, triazoles, triazines, or quinoxalines,[43] but molecules such as fluorenone, containing the ketone functionality, may also display electron transport capability.[44,45]

Acknowledgment. This work was supported by a National Research Council/National Science and Engineering Research Council of Canada, Research Partnership Project Grant involving Luxell Technologies.

Supporting Information Available: Detailed experimental procedure used to synthesize CH, A435, and STPD-QP; synthesis of the high T_g amorphous poly(imidoaryl ether sulfone) CH; synthesis of the high T_g amorphous poly(aryl ether ketone) A435; synthesis of 4,4‴-dihydrozy-*p*-quaterphenyl; preparation of blue light emitting polymer STPD-QP; figure of the surface morphology of various films (PDF). This material is available free of charge via the Internet at http://pubs.acs.org.

CM0009221

(43) Thelakkat, M.; Schmidt, H. W. *Polym. Adv. Technol.* **1998**, *9*, 429.
(44) Uckert, F.; Tak, Y. H.; Müllen, K.; Bässler, H. *Adv. Mater.* **2000**, *12*, 905.
(45) Katz, H. E.; Lovinger, A. L.; Johnson, J.; Kloc, C.; Siegrist, T.; Li, W.; Lin, Y. Y.; Dodabalapur, A. *Nature* **2000**, *404*, 478.